

ENCLOSURES

THE EFFECT OF ENCLOSING A TRANSDUCER

5.1 The Simple Closed Box

In order to understand the effect of an enclosure it is instructive to derive the simplest form of an enclosure directly from the principles that we have already learned, namely the Wave Equation. We will then move on to the T-matrix approach showing the near equivalence of the two. In this way we will learn how to combine the continuous nature of sound radiation with the more discrete (i.e. lumped parameter or T-matrix) nature of the enclosure problem.

Consider a spherical enclosure with a piston set in it. We have already learned how the sound radiates from the outside of this enclosure. Now we want to determine the effect the inside of the enclosure will have on the transducer. In order to do this we must once again return to the equations of Secs. 3.4 and 3.5. In those sections we used Bessel Functions which are appropriate for external sound radiation, namely the Spherical Hankel Functions. We must now consider the solutions to the Spherical Wave Equation that are appropriate to the interior standing wave problem.

The appropriate set of functions for the interior problem are known to be the Spherical Bessel Functions of the first and second kinds

$$p(r) = A_m j_m(kr) + B_m n_m(kr) \quad (5.1.1)$$

$j_m =$ the Spherical Bessel Function of the first kind

$n_m =$ the Spherical Bessel Function of the second kind

The solution to the problem that we are currently considering, the interior of a spherical shell, must be analytic (finite) within this shell, which also contains the origin. Therefore we can exclude the second function since it is singular at the origin. There are cases, such as a spherical shell with an inner rigid sphere which contains the origin, for which this simplification is not possible. It is wise not to assume that we can always exclude the singular solution.

The boundary conditions that we have for this problem are

$$v(r, \theta) \Big|_{r=a} = \begin{cases} v_0 & \theta < \theta_0 \\ 0 & \text{otherwise} \end{cases} \quad (5.1.2)$$

The general solution then becomes

$$p(r, \theta) = \sum_m A_m j_m(kr) P_m(\cos \theta) \tag{5.1.3}$$

which must equal the boundary conditions specified in (Eq.(5.1.2)). Proceeding identically to the examples that we have used before, we will find

$$\sum_m A_m P_m(\cos \theta) j_m'(ka) = -i \rho c V(\theta) \tag{5.1.4}$$

and by applying the conditions of orthogonality we have

$$-i \rho c \int_{-1}^1 V(\theta) \cdot P_m(\mu) d\mu = \sum_m A_m \int_{-1}^1 P_m(\mu) \cdot P_n(\mu) d\mu j_m'(ka) \tag{5.1.5}$$

and finally

$$A_m = -i \rho c \frac{(n + \frac{1}{2})}{j_m'(ka)} \int_{-1}^1 V(\theta) \cdot P_m(\mu) d\mu \tag{5.1.6}$$

In order to calculate the impedance seen by the source we must integrate this pressure response over the area of the source.

$$z_a = \frac{\pi r^2}{S_d^2} \int_0^{\theta_0} p(\theta) P_m(\cos \theta) \sin \theta d\theta \tag{5.1.7}$$

$S_d =$ the area of the piston

The division by S_d^2 is required to yield the acoustical impedance.

Fig.5-1 shows the impedance seen by the source in Acoustical Ohms for a sphere of volume $V = \frac{4}{3} \pi r^3 = .25 m^3$ with a source of radius $a_p = 7.8$ cm. These dimensions correspond (approximately) to an eight inch loudspeaker in a 25 liter box.

From the figure we can see that the impedance is actually quite complex at the higher frequencies, corresponding to the internal box resonances. Below the first resonance, however, the curve appears to be a simple compliance in series with a lumped mass. For this example, the acoustic compliance and mass of the interior impedance are found to be

$$C_a = \frac{\rho c^2}{V_s} \tag{5.1.8}$$

$$M_a = .85 \frac{\rho}{\pi a_p}$$

$C_a =$ acoustic compliance,

$M_a =$ acoustic mass.

Note that at the box “anti-resonance” the box does not even appear to be present. At the higher frequencies we get into a multiplicity of box resonances

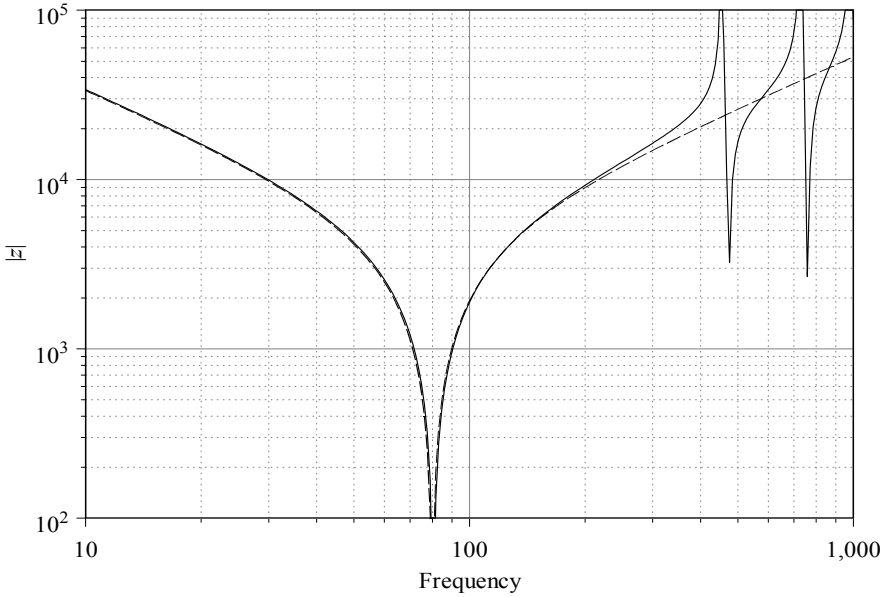


Figure 5-1 - Acoustical impedance of a sphere

which could present some problems. We will now add some damping to the walls to see if we can get rid of the resonances, or at least reduce them.

In the damped case we must have a different boundary condition, namely

$$z = \frac{v(r, \theta)}{p(r, \theta)} \Big|_{r=a} = \alpha \quad (5.1.9)$$

$z = \alpha$ = the value of the impedance at the walls.

The value of α is assumed here to be real (absorptive). We could just as easily have allowed the walls to be flexible, but that is not usually the way enclosures are made. Using the new form we have

$$\frac{-i \rho c \sum_m A_m j_m'(ka) P_m(\cos \theta)}{\sum_m B_m P_m(\cos \theta) j_m(ka)} = \alpha \quad (5.1.10)$$

From this equation we can conclude that the Eigenfunctions in this space must be of the form

$$j_m'(ka) + \frac{\alpha}{i \rho c} j_m(ka) = 0 \quad (5.1.11)$$

in order to satisfy the boundary conditions.

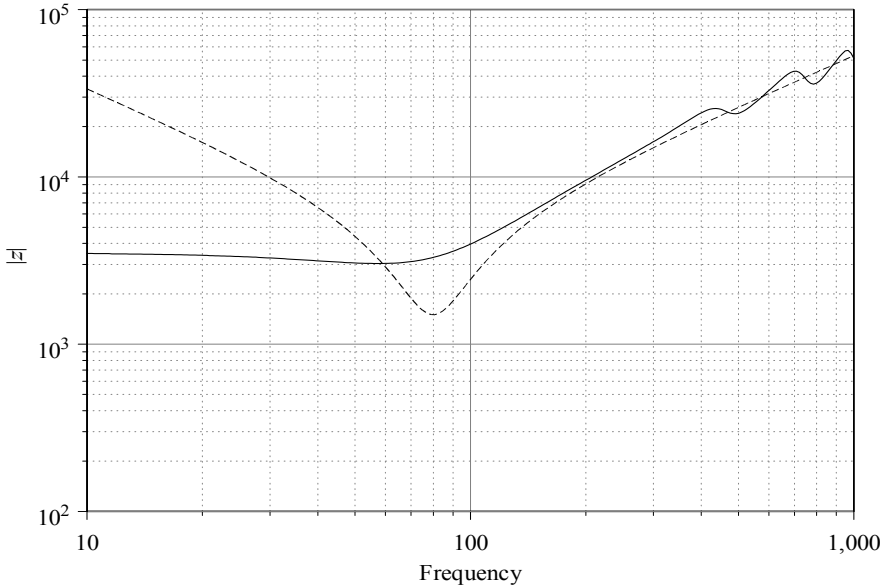


Figure 5-2 - Closed spherical box with inner wall impedance $\alpha=.15$

The solution to our problem then is really quite straightforward. In Eq. (5.1.3) we simply substitute the wave functions used in that equation ($j'_m(ka)$ in that case) with the new wave functions - the functions which satisfy the new boundary conditions.

An example of this calculation is shown in the figure above. We can immediately see that this result is unrealistic since it appears to completely negate the enclosed compliance of the air. This problem is caused by the fact that, in reality, it is impossible to achieve an actual value of wall impedance which is constant with frequency. The impedance must disappear as the frequency is lowered since the velocity goes to zero.

A more realistic approach is to use a wall impedance that vanishes at low frequencies and asymptotically approaches its maximum value at high frequencies. Using this new impedance function we get the curves shown in Fig 5-3. This result is much more satisfying, but we can improve upon it even more.

We can see that the low frequency fit to an equation form which consists of a compliance, a mass and a resistance all in series over estimates the compliance at the low end of the spectrum. This is true because of (or as a result of) the fact that the impedance disappears in this region. By adjusting the volume with a term which depends on α 's asymptotic value

$$V_{\text{mod}} = 1 + 2\alpha^2 \tag{5.1.12}$$

we can achieve the results shown in Fig 5-4. The match between the analytical calculation and the lumped parameter form are now quite similar. It is of course well

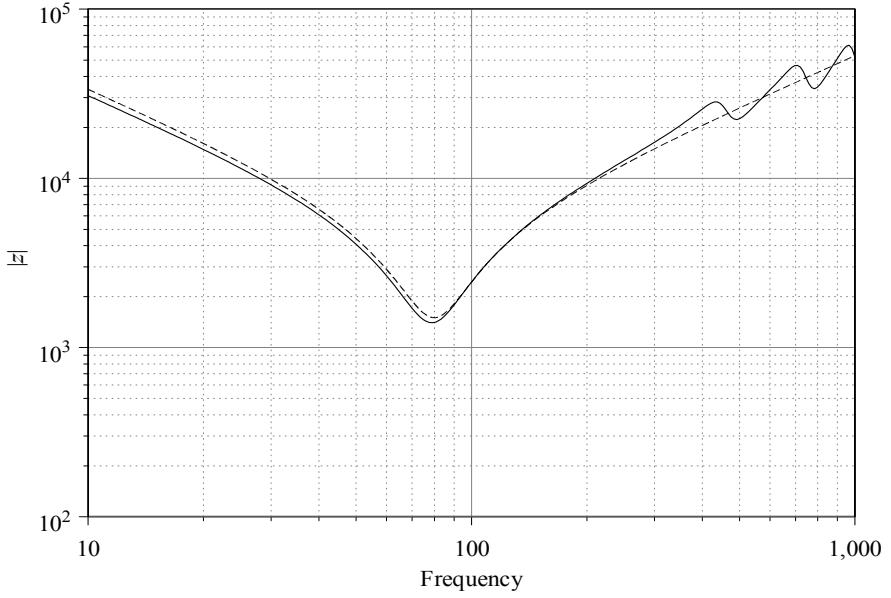


Figure 5-3 - Fig.5-4 with a more realistic wall impedance

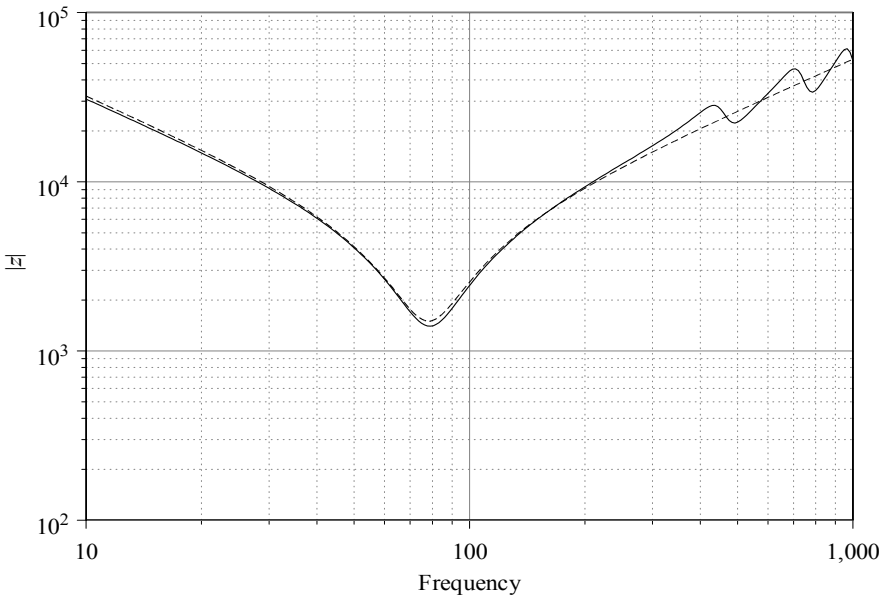


Figure 5-4 - Closed sphere with corrected apparent volume

know that the apparent volume of a box increase with the addition of absorption. However, the reasons usually given for this effect are that it is due to the difference between isothermal and adiabatic wave propagation. Note that we have obtained a comparable result without the need for this explanation. In our analysis, the increase in apparent volume is simply a result of the fact that there is damping that vanishes at low frequencies. It may well be that the two explanations are simply semantic and are really one and the same. This different point of view will not be resolved here since general acoustics (including molecular considerations) is not really the focus of this text. It is sufficient for us to note that either approach leads to the same result – that the apparent volume increases with increased damping and that with sufficient damping the impedance presented to the transducer by the enclosed space is represented quite accurately by a simple three parameter model.

One more aspect of this problem should be mentioned. There is another way to approach the evaluation of the damping problem. The other approach is to assume a continuous (in space) form of damping by letting the wavenumber k be represented as a complex quantity

$$k = \frac{\omega}{c}(1 + i\alpha) \quad (5.1.13)$$

This approach to damping is called structural damping in mechanics. It occurs when wave motion in the medium causes energy dissipation, such as would happen with a distributed material like fiberglass. Note that this form of damping naturally rises with frequency, which we know to be true at low frequencies. In the above equation however it continues to rise with frequency, which is not always the case. Air absorption has does have this form, continuously increasing with frequency throughout the audible range, but starting at a very low value of sound absorption in the lower frequencies. It is likely that a real enclosure with distributed damping material could best be fit by both solutions – continuous damping and wall impedance damping.

The problem, the use of a complex value for k , as suggested above, can be solved, but it requires that one be able to evaluate Bessel Functions of an imaginary argument. Computer subroutines to do this evaluation are readily available¹, but their usage is beyond the scope of this book. Further, the results would be nearly the same as what we have already shown. We bring this up now because in the next section we will once again consider the use of a complex wavenumber. The functions that we will be using there are, however, much simpler than Bessel Functions and the values for complex arguments are well know.

1. See Zhang and Jin, *Computation of Special Functions*.

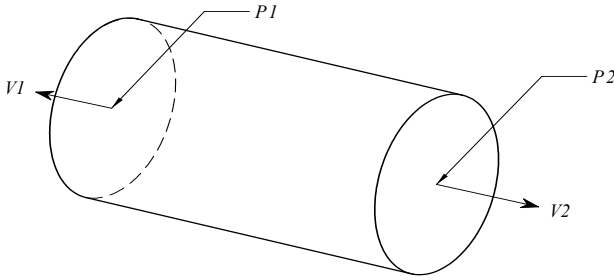


Figure 5-5 - One dimensional cylinder with two ports

5.2 An Enclosure in T-matrix Format

We will now take what might appear to be a sideline from our study, however the discussion does come back around to mesh with the previous section discussion.

Consider the problem of a one dimensional cylinder as shown in the figure above. It is one dimensional because we will not consider cross modes. We want to find the T-matrix representation of this element.

From Sec.3.2 we know that the solution to the one dimensional Wave Equation in Rectangular Coordinates is

$$\phi(x) = A e^{i(\omega t - kx)} + B e^{i(\omega t + kx)} \quad (5.2.14)$$

which represents waves moving in both the positive and negative x directions. Here $\phi(x)$ is the velocity potential function. Applying this form to the two faces of the duct we have

$$\begin{aligned} p(x) &= \rho \frac{d}{dt} \phi(x) = i\omega \rho e^{-ikx} A + i\omega \rho e^{ikx} B \\ v(x) &= \frac{d}{dx} \phi(x) = -ik e^{-ikx} A + ik e^{ikx} B \end{aligned} \quad (5.2.15)$$

Written in a more convenient form this equation becomes

$$\begin{pmatrix} p(x) \\ v(x) \end{pmatrix} = \begin{bmatrix} i\omega \rho e^{-ikx} & i\omega \rho e^{ikx} \\ -ike^{-ikx} & ike^{ikx} \end{bmatrix} \begin{pmatrix} A \\ B \end{pmatrix} \quad (5.2.16)$$

We can apply this equation to both ends of the duct to yield two matrices

$$\begin{pmatrix} p_1 \\ v_1 \end{pmatrix} = \begin{bmatrix} i\omega \rho e^{-ikx_1} & i\omega \rho e^{ikx_1} \\ -ike^{-ikx_1} & ike^{ikx_1} \end{bmatrix} \begin{pmatrix} A \\ B \end{pmatrix} = [T(x_1)] \begin{pmatrix} A \\ B \end{pmatrix} \quad (5.2.17)$$

and

$$\begin{pmatrix} p_2 \\ v_2 \end{pmatrix} = \begin{bmatrix} i\omega \rho e^{-ikx_2} & i\omega \rho e^{ikx_2} \\ ike^{-ikx_2} & -ike^{ikx_2} \end{bmatrix} \begin{pmatrix} A \\ B \end{pmatrix} = [T(x_2)] \begin{pmatrix} A \\ B \end{pmatrix} \quad (5.2.18)$$

Note that in this later equation the velocity is in the opposite direction from the velocity at the other end of the duct, as in the previous equation.

We can now solve for the vector $(A B)$ in both equations and set them equal to each other

$$\begin{pmatrix} p_1 \\ v_1 \end{pmatrix} = [T(x_1)][T(x_2)]^{-1} \begin{pmatrix} p_2 \\ v_2 \end{pmatrix} \tag{5.2.19}$$

which will yield the result that we want

$$\begin{pmatrix} p_1 \\ V_1 \end{pmatrix} = \begin{bmatrix} \cos(kL) & \frac{-i\rho c}{A} \sin(kL) \\ \frac{A \sin(kL)}{i\rho c} & \cos(kL) \end{bmatrix} \begin{pmatrix} p_2 \\ V_2 \end{pmatrix} \tag{5.2.20}$$

$L = x_2 - x_1$, the length of the duct

$A =$ the area of the duct

The area was introduced to convert the particle velocity into the volume velocity, which is the variable that we will use in the acoustic domain. Eq.(5.2.20) is a convenient and simple result. This equation represents the core T-matrix for the acoustical domain in the T-matrix modeling approach that we use in this text. It can be adopted to handle nearly every component that we will encounter in the acoustic domain where free sound radiation is not possible. We will now look at a few examples of its usefulness and then we will extend its accuracy.

5.3 T-matrix and Lumped Parameter

The T-matrix approach lies between the lumped parameter approach commonly used for transducer design and the Wave Equation approach shown in the first section of this chapter. It is more broadly applicable than lumped parameter, but more limiting than the Wave Equation. Let's look at how the lumped parameter forms for acoustic elements are subsets – simplifications – of the T-matrix approach.

Consider a transducer in the end of a tube of length L , and closed at the other end. Eq.(5.2.20) becomes, for the acoustic variables presented to the transducer at point 1,

$$\begin{aligned} p_1 &= \cos(kL)p_2 - i \frac{\rho c}{A} \sin(kL)V_2 \\ V_1 &= -i \frac{A}{\rho c} \sin(kL)p_2 + \cos(kL)V_2 \end{aligned} \tag{5.3.21}$$

To find the impedance presented to the source we set $V_2=0$, which represents a closed end, and then we divide the resulting equation for p_1 by the equation for V_1

$$z_1 = \frac{p_1}{V_1} = \frac{-i\rho c \cos(kL)}{A \sin(kL)} = \frac{-i\rho c}{A} \cot(kL) \quad (5.3.22)$$

Fig.5-6 shows the acoustical impedance seen by a transducer in the end of a closed duct, using the same piston area and volume as the previous example (Fig.5-1 on page 91). We can see that the comparison is good up to just above

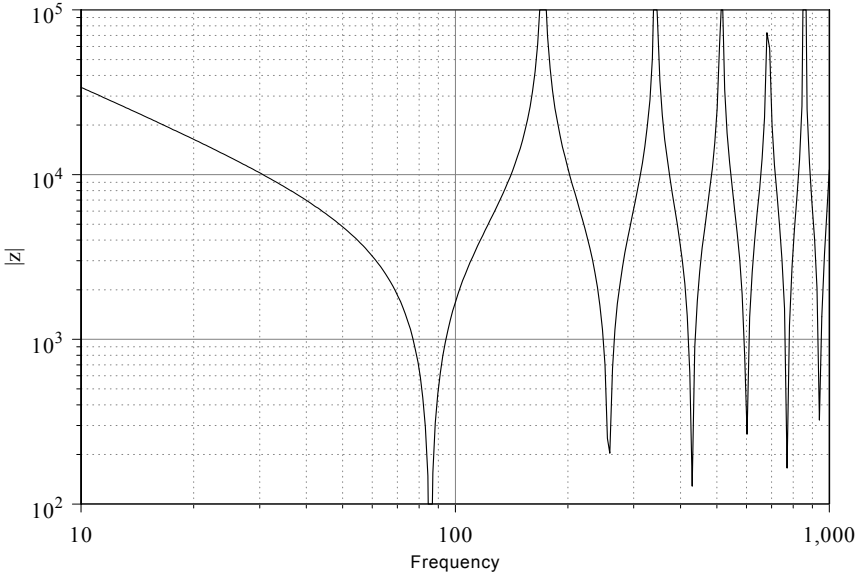


Figure 5-6 - Acoustical impedance load on a transducer in the end of a closed duct

100 Hz, after which the cylindrical enclosure has a much higher density of modes and there is no apparent rise in the mean impedance level with frequency – the internal mass effect.

If we look at Eq.(5.3.22) for small kL we find that

$$z = \frac{i\rho c}{AkL} = \frac{\rho c^2}{-i\omega V} \quad (5.3.23)$$

Further if we look at Eq.(5.3.21) for small kL we find

$$\begin{bmatrix} 1 & 0 \\ -i\omega \frac{V}{\rho c^2} & 1 \end{bmatrix} \quad (5.3.24)$$

which is the T-matrix for a capacitor to ground with a value of $V/\rho c^2$, the lumped parameter result.

Thus we have shown that the T-matrix is more broadly applicable than the lumped parameter model, but we must also remember that it is not always exactly

correct. That is, the matrix form should be expected to be correct for an enclosure with dimensions such that it is a long tube with a cross sectional area equal to the area of the transducer, which is placed in one end. This is a close approximation to the common design of a “tower” cabinet with the woofer at the top or the bottom. We will now see how to make this analysis even more accurate.

If we place damping material at the closed end of the enclosure then we will have an impedance boundary condition, instead of a zero velocity boundary condition. In this case Eq.(5.3.21) becomes

$$z_1 = \frac{p_1}{V_1} = \frac{\cos(kL)p_2 + \frac{-i\rho c}{A}\sin(kL)V_2}{\frac{A}{i\rho c}\sin(kL)p_2 + \cos(kL)V_2} = \frac{z_2 - \frac{i\rho c}{A}\tan(kL)}{1 + \frac{z_2 A}{i\rho c}\tan(kL)} \tag{5.3.25}$$

but an easier way to get the same result (calculations show that both methods give the same results for “typical” cases) is to use the structural damping model shown in the previous section. In this model we simply let the wavenumber be complex. The impedance has the same form as that above except that k is now given by Eq.(5.1.13). Fig.5-7 shows the impedance function for a value of $\eta = .25$.

The T-matrix form has the correct characteristics, i.e. similar to the exact Wave Equation formulation, up until about the first mode in the duct. After this point the impedance does not have the correct value of mass reactance. This is to be expected. Since to be exactly correct the driver in our example would have the same radius as the duct, there would be no divergence of the wavefront (spherical

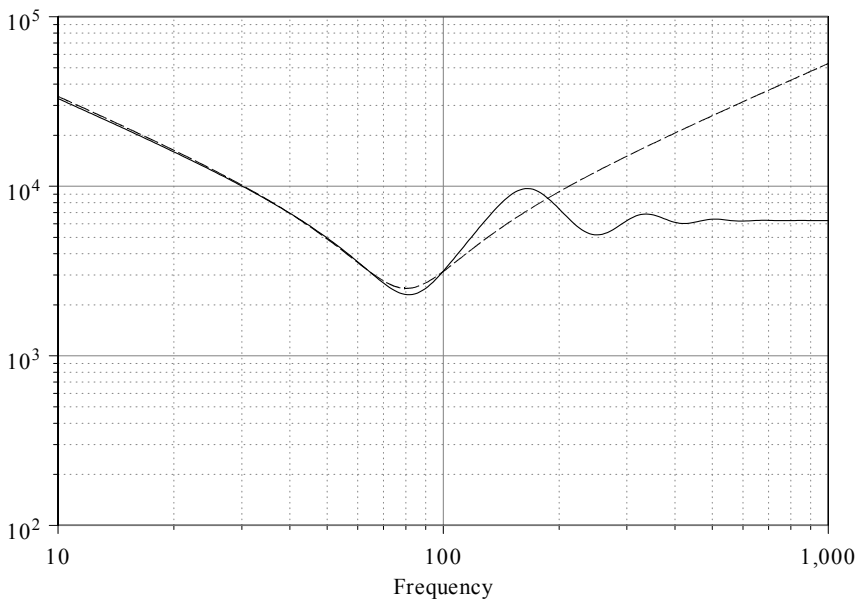


Figure 5-7 - T-matrix impedance with complex k and lumped parameter results

spreading) and hence no acoustic mass – exactly what we have found! The spherical enclosure does have spherical spreading and as such does exhibit an internal mass effect.

Consider now a duct that is open at the un-driven end. This is a pressure release boundary condition and we must have (to a first order) $p_2=0$, resulting in

$$z = \frac{p_1}{V_1} = \frac{-i\rho c}{A} \frac{\sin(kL)}{\cos(kL)} = -\frac{i\rho c}{A} \tan(kL) \quad (5.3.26)$$

A plot of this impedance is shown in Fig.5-8. This figure indicates that a duct works as a lumped mass only in the low frequency region. Once standing waves begin to occur, it is hardly a simple lumped mass.

When kL is small, the T-matrix in Eq.(5.3.21) becomes

$$\begin{bmatrix} 1 & -i\omega \frac{\rho L}{A} \\ -i\omega \frac{V}{\rho c^2} & 1 \end{bmatrix} \quad (5.3.27)$$

which for a tube of large length to width ratio is approximately that of a series mass with a value $r L/A$, the known lumped parameter result. The results shown in Eq.(5.3.27) point out an interesting characteristic of ducts. The duct works as

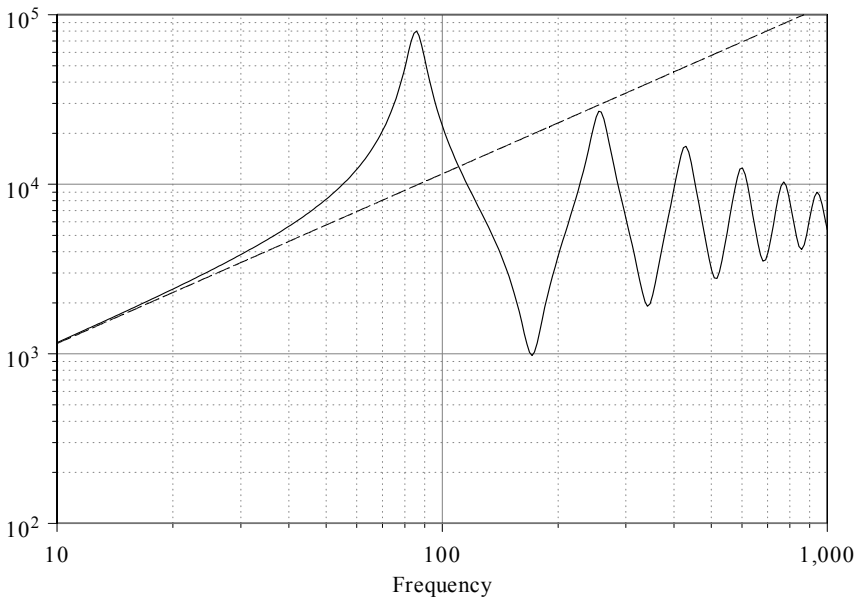


Figure 5-8 - Impedance of an open tube load with a radiation impedance

both a mass and compliance. Only when the load impedance is negligible, i.e. $p_2 = 0$, does a duct behave like a pure acoustic mass.

We can see that the single T-matrix for a duct can represent all of the lumped parameter elements that we usually require and it does so with a greater accuracy than the lumped parameter forms. We should also mention that the wave functions for other coordinates could be used in the derivation of the T-matrix as shown in Sec. 5.2. For instance, spherical wave functions, which are also quite simple (see Sec. 3.2) could be used to develop the T-matrix for a tapered rear enclosure, such as that found in some loudspeaker systems. By using a complex wavenumber, an accurate equation for this style of enclosure, when stuffed with damping material, could be calculated. There is, in fact, no limit to the applicability of this approach to any of the orthogonal coordinate systems. Yet another reason for our appreciation of them.

5.4 A Ported Enclosure Using T-Matrices.

In order to show how T-matrices can be used for both analytical as well as numerical analysis, a specific example of a simple rear ducted enclosure will be shown. The techniques that we will use in this section are applicable to any enclosure design and will be the basis for our later discussions of enclosures. In this section, we will do a detailed analysis of the sound radiation from a duct ported enclosure in order to compare the T-matrix approach with the lumped parameter approach. This problem was chosen since it tends to maximize the differences in the two derivations. We will then use the T-matrix approach in later sections, where we will do a “results only” analysis of more complex enclosure types.

In this text the term port means an opening in an enclosure, consistent with the dictionary definition. A port can have any of several different objects in it, the simplest being a duct or simple tube.

A convenient way to look at a rear ducted system is as shown in Fig. 5-9. This figure has two tubes, linked together at the rear with a “port” of the same area as the duct, A_d . The first tube has area A_e , is also of length L and has a transducer of

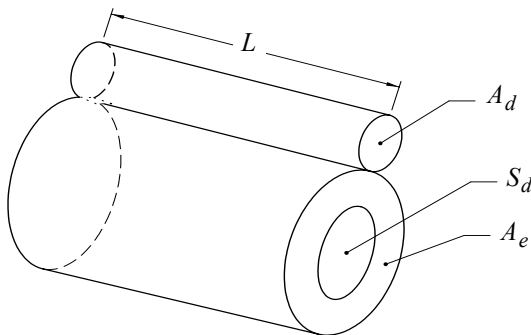


Figure 5-9 - Rear ducted enclosure of conventional design

area S_d placed in the end opposite the port. The radiated output is the of the sum of the volume velocities of S_d and A_d . Enclosures like these are common in the marketplace.

The T-matrices are linked together just as they appear in the drawing.

$$\begin{bmatrix} E(\omega) \\ I(\omega) \end{bmatrix} = \begin{bmatrix} 1 & z_e \\ 0 & 1 \end{bmatrix} \begin{bmatrix} 0 & Bl \\ Bl^{-1} & 0 \end{bmatrix} \begin{bmatrix} 1 & -i\omega M_m + R_m + \frac{1}{-i\omega C_m} \\ 0 & 1 \end{bmatrix} \begin{bmatrix} S_d & 0 \\ 0 & S_d^{-1} \end{bmatrix} \begin{bmatrix} P_d \\ V_d \end{bmatrix} \quad (5.4.28)$$

$$\begin{bmatrix} \cos(kL) & \frac{-i\rho c}{A_e} \sin(kL) \\ \frac{A_e \sin(kL)}{i\rho c} & \cos(kL) \end{bmatrix} \begin{bmatrix} \cos(kL) & \frac{-i\rho c}{A_d} \sin(kL) \\ \frac{A_d \sin(kL)}{i\rho c} & \cos(kL) \end{bmatrix} \begin{bmatrix} P_d \\ V_d \end{bmatrix}$$

The driver matrices are the top row and the enclosure is the bottom row. This equation contains a new matrix that we have not seen before. It is the diagonal matrix with S_d in the terms. This matrix represents the change from the mechanical domain into the acoustical domain and has the form of a transformer. The conversion from the mechanical to acoustical domains is quite simple in this model, but in general it can get quite complex (a non-rigid cone for instance).

This seems a rather laborious result, and not at all instructive, but we must keep in mind that Eq.(5.4.28) contains all of the information that can be know about this system (at least to the order of the model). It is applicable to any situation; a current source, a voltage source or mixed source conditions and the load impedances can be any value – a very broad range of applicability. By making a few simplifications we will see that it readily becomes more manageable.

First consider a voltage source and a negligible acoustical load impedance (the same approximations assumed by Thiele, Small, etc.). Further assume that kL is small in all terms and discard the insignificant ones (as we did in the previous section). Consider the electrical impedance as only R_e .

If we apply these limitations and multiply out the terms we get

$$\frac{E(f)}{V(f)} \cdot \frac{i\omega Bl C_m}{S_d R_e} = \quad (5.4.29)$$

$$M_{as} C_{as} M_{ad} C_e \cdot \omega^4 - iR_t C_{as} C_e M_{ad} \omega^3 + (M_{as} C_{as} - M_{ad} C_e) \omega^2 - iR_t C_{as} \omega - 1$$

$$R_t = R_{as} + \frac{Bl^2}{R_e S_d^2} \quad C_e = \frac{A_e L}{\rho c^2} \quad M_{ad} = \frac{\rho L}{A_d}$$

The transducer parameters used here have all of been converted to acoustical quantities by multiplying their impedances by S_d^2 .

Using the standard definitions

$$\begin{aligned}
 M_{as}C_{as} &= \frac{1}{\omega_s^2}, \\
 M_{ad}C_e &= \frac{1}{\omega_b^2}, \\
 R_tC_{as} &= \frac{1}{\omega_s Q_t}
 \end{aligned}
 \tag{5.4.30}$$

and rewriting Eq.(5.4.29) we get for the volume velocity of the free end of the duct

$$V(f) = \frac{i\omega \frac{BlC_{as}}{S_d R_e} \cdot E(f)}{\left(\frac{\omega^4}{\omega_s^2 \omega_b^2} - i \frac{\omega^3}{Q_t \omega_s \omega_b^2} + \omega^2 \left(\frac{1}{\omega_s^2} - \frac{1}{\omega_b^2} \left(1 - \alpha \left(1 + \frac{A_d}{A_e} \right) \right) \right) - i \frac{\omega}{Q_t \omega_s} + 1 \right)}
 \tag{5.4.31}$$

which agrees with the lumped parameter analysis.

The results of this equation are shown in Fig 5-10 along with the more accurate T-matrix results (which are too complex to write out). This curve suggests

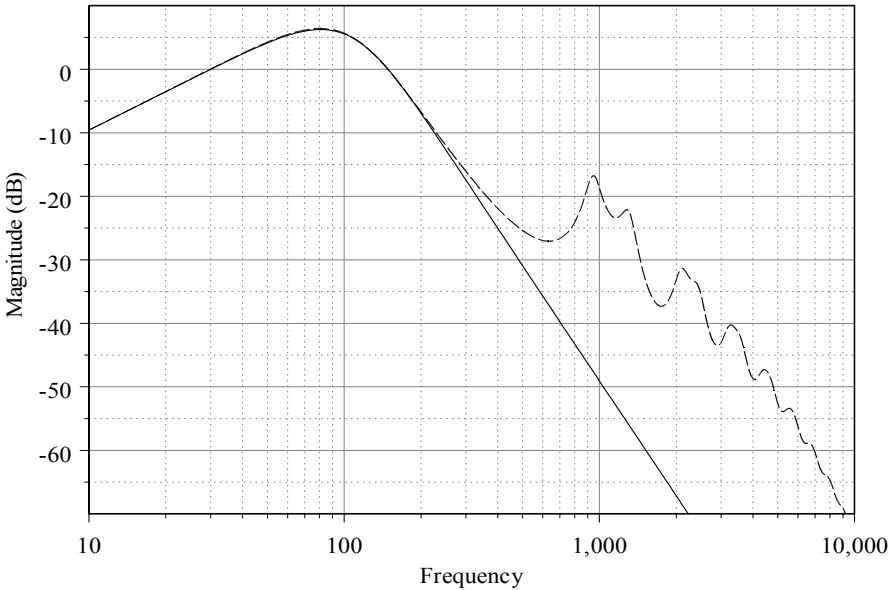


Figure 5-10 - Comparison of lumped parameter versus T-matrix for duct velocity

that there is little difference between the two, although this conclusion would be in error. It is important to reiterate that what we have derived here is the volume

velocity of the duct radiation not the complete sound radiation. Also, we have not yet considered the radiation from the transducer.

(All of the curves shown in this section have had a small amount of damping added to the wavenumber to reduce the peak resonance values. This would occur in a typical enclosure with damping in it and is felt to be realistic.)

5.5 The Mechanical Acoustical Interface

In order to calculate the result of a combined loudspeaker and duct radiation we will have to examine the T-matrix approach in some more detail.

In reality, the loudspeaker is not a simple two-port system. It has a single input, but it has two outputs, the front and rear of the diaphragm, although it is important to note that they are not completely independent. The acoustic volume velocity on each side of the diaphragm is the same, but the pressure is not (the impedance seen by each side of the diaphragm can be different). The analysis thus contains a center tapped transformer known as bifilar – both legs have equal and opposite currents. We can demonstrate this with the following constraint equations on the mechanical acoustical interface

$$\begin{aligned} F_d &= P_f S_d - P_r S_d \\ v_d &= \frac{V_f}{S_d} \\ v_d &= \frac{V_r}{S_d} \end{aligned} \tag{5.5.32}$$

P_f = the pressure on the front of the diaphragm

P_r = the pressure on the rear of the diaphragm

V_f = the volume velocity of the rear

V_r = the volume velocity of the rear

S_d = the diaphragm area

The representation of these equations is

$$\begin{pmatrix} F_d \\ v_d \\ v_d \end{pmatrix} = \begin{bmatrix} S_d & 0 & -S_d & 0 \\ 0 & 1/S_d & 0 & 0 \\ 0 & 0 & 0 & -1/S_d \end{bmatrix} \begin{pmatrix} P_f \\ V_f \\ P_r \\ V_r \end{pmatrix} \tag{5.5.33}$$

which is an over determined set with the variable v_d appearing twice. This over-determination is necessary when one actually goes to calculate values, since it will be used to eliminate one of the output variables. For example, consider the following case.

When there are arbitrary T-matrices on the front and rear, then we would get the following situation

$$\begin{pmatrix} F_d \\ v_d \\ v_d \end{pmatrix} = \begin{bmatrix} S_d & 0 & -S_d & 0 \\ 0 & 1/S_d & 0 & 0 \\ 0 & 0 & 0 & -1/S_d \end{bmatrix} \begin{bmatrix} Z_f^{1,1} & Z_f^{1,2} & 0 & 0 \\ Z_f^{2,1} & Z_f^{2,2} & 0 & 0 \\ 0 & 0 & Z_r^{1,1} & Z_r^{1,2} \\ 0 & 0 & Z_r^{2,1} & Z_r^{2,2} \end{bmatrix} \begin{pmatrix} P_f \\ V_f \\ P_r \\ V_r \end{pmatrix} \tag{5.5.34}$$

Z_f = the front composite T-matrix

Z_r = the rear composite T-matrix

where the output variables now refer to the system output. This equation is not the most general form since it assumes no coupling between the front and rear of the diaphragm internal to the system. We will investigate a modification to this assumption later. The acoustical T-matrices are linked as sub-matrices of the more general 4 x 4 matrix. This approach is perfectly correct and accurate, but it can get to be inefficient in storage and calculation requirements, especially since there are only a few situations that actually require this full matrix representation. Multiply out the above form to yield

$$\begin{pmatrix} F_d \\ v_d \\ v_d \end{pmatrix} = \begin{bmatrix} S_d Z_f^{1,1} P_f + S_d Z_f^{1,2} V_f - S_d Z_r^{1,1} P_r - S_d Z_r^{1,2} V_r \\ \frac{Z_f^{2,1} P_f}{S_d} + \frac{Z_f^{2,2} U_f}{S_d} \\ \frac{Z_r^{2,1} P_r}{S_d} + \frac{Z_r^{2,2} U_r}{S_d} \end{bmatrix} \tag{5.5.35}$$

An investigation of this equation reveals that only one of these equations is coupled (front to rear) and then only as a sum (difference) of uncoupled terms. This means that if there is no direct link from the front of the diaphragm to the rear then there is no need for the more general 4 x 4 matrix approach. The solution can be found by considering either velocity equation and taking the force as the sum of the forces on the front and rear. This reduces the problem to a standard 2 x 2 system.

As an example, consider the case where we have a diaphragm that is direct radiating on the front and has a closed box placed on the rear. The front T-matrix will be an identity matrix and the rear matrix will be as shown in Eq.(5.3.27). With $V_r = 0$. Eq.(5.5.35) then becomes

$$\begin{pmatrix} F_d \\ v_d \\ v_d \end{pmatrix} = \begin{bmatrix} S_d P_f - S_d P_r \\ U_f / S_d \\ -i\omega V P_r / (\rho c^2 S_d) \end{bmatrix} \tag{5.5.36}$$

which appears to simply be a restatement of the fundamental relationships shown in Eq.(5.5.32), except for the bottom equation, which must also be true. We can use this equation to eliminate P_r in the top equation and then simply drop the last equation (since we have already used it). Doing this we get

$$\begin{pmatrix} F_d \\ v_d \end{pmatrix} = \begin{bmatrix} S_d & \frac{S_d \rho c^2}{i\omega V} \\ 0 & 1/S_d \end{bmatrix} \begin{bmatrix} P_f \\ U_f \end{bmatrix} = \begin{bmatrix} 1 & \frac{S_d^2 \rho c^2}{i\omega V} \\ 0 & 1 \end{bmatrix} \begin{bmatrix} S_d & 0 \\ 0 & 1/S_d \end{bmatrix} \begin{bmatrix} P_f \\ U_f \end{bmatrix} \quad (5.5.37)$$

If we add the mechanical matrix for the diaphragm on the left hand side and multiply both sides by the inverse of the first matrix on the right hand side we will get

$$\begin{bmatrix} 1 & \frac{S_d^2 \rho c^2}{-i\omega V} \\ 0 & 1 \end{bmatrix} \begin{bmatrix} 1 & z_m \\ 0 & 1 \end{bmatrix} \begin{pmatrix} F_d \\ v_d \end{pmatrix} = \begin{bmatrix} 1 & z_m + \frac{S_d^2 \rho c^2}{-i\omega V} \\ 0 & 1 \end{bmatrix} \begin{pmatrix} F_d \\ v_d \end{pmatrix} \quad (5.5.38)$$

$$= \begin{bmatrix} S_d & 0 \\ 0 & 1/S_d \end{bmatrix} \begin{bmatrix} P_f \\ U_f \end{bmatrix}$$

which can be seen to be the correct result, where the rear enclosure volume simply adds its mechanical compliance to the drivers compliance.

In summary, by simply calculating the front and rear T-matrices as separate paths we can combine their effects on the diaphragm by summing them into a single complex impedance load to the mechanical system. This reduces the acoustical domains calculation load by about four times – a significant factor for little loss in generality and no loss in accuracy. A case where we cannot make this simplification will be shown in the section “Internal Ported” on page 123.

5.6 Front and Rear Port Radiation

Returning now to the ducted enclosure we can calculate the load presented to the rear diaphragm (the only load if we ignore the radiation load, which is negligible.) We can then calculate the cone velocity and simply multiply by the radiation area to get the volume velocity. We can then add the two results (actually subtract) to find the total volume velocity. By making a simple scalar sum of the radiating volume velocities we have assumed that the duct and loudspeaker are close together. In the example that we are studying they are close together, but if they were farther apart then we would have to sum the actual radiated pressure instead of the near field volume velocity. There are cases where this difference can be quite significant.

The results of the calculations are shown in Fig.5-11. This figure shows the loudspeakers radiated pressure and the total radiated pressure for both the lumped parameter and the T-matrix calculations. There is about a 2 dB difference up to almost 1 kHz. where the differences become very large. The reason for this discrepancy can be seen in Fig 5-12. This figure shows the lumped parameter acoustic impedance of the enclosure versus the T-matrix calculation of the same enclosure. The T-matrix calculation is predicting much smaller impedance values in the range just above resonance. The T-matrix calculations are more accurate in this region.

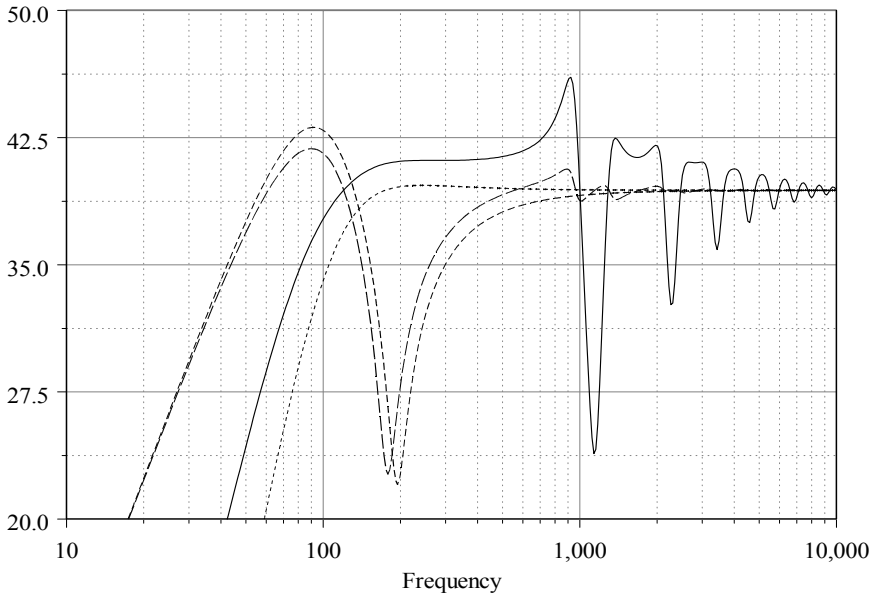


Figure 5-11 - Simulated pressure response for lumped parameter and T-matrix calculations

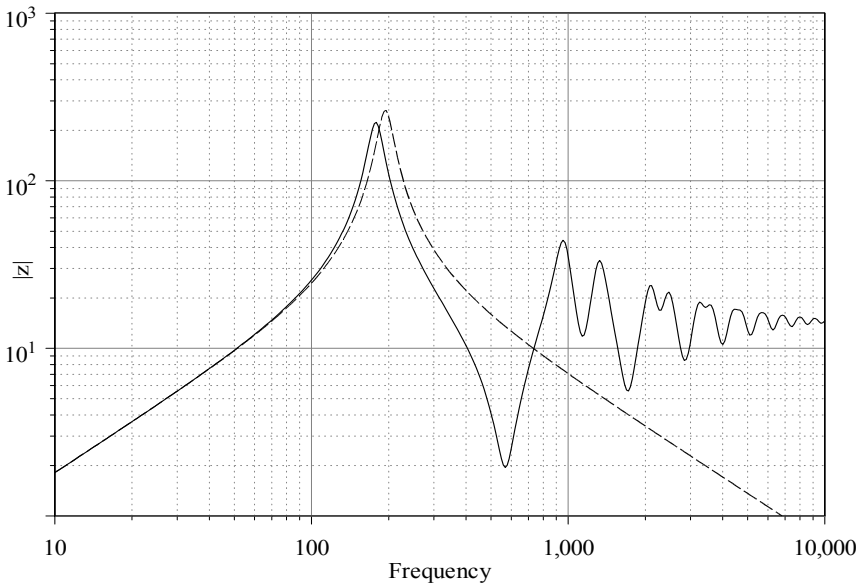


Figure 5-12 - Acoustic impedance of the enclosure for lumped parameter and T-matrix

We will now calculate a simple iteration of the length of the enclosure just to show the effect. Remember that, in this system, as the duct gets longer the net enclosure volume also increases at the same time – the duct and the enclosure have a common length. The results are shown in Fig.5-13 for lengths of .1m, .12m and .15m. The common length of the two tubes in this system makes the resonance frequencies in the duct and the enclosure common, which accounts for the pronounced effect of these higher order modes.

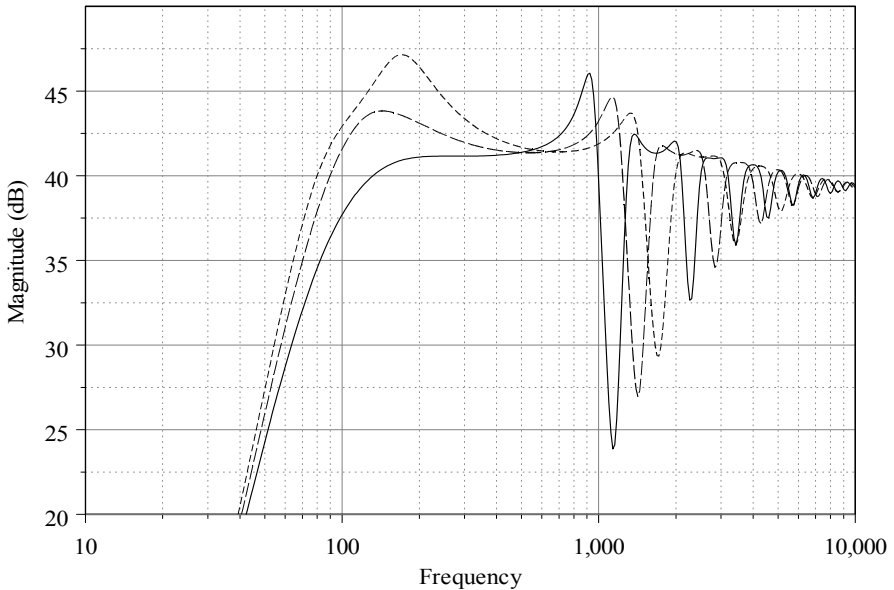


Figure 5-13 - Iteration of common length of box and duct.

Lastly, consider the fact that the duct radiation is exactly the same radiation that would occur for a single ported bandpass system (except that the driver parameters would then be those of the driver in its rear enclosure, not in free space.) Fig.5-10 then also shows the results of T-matrix versus lumped parameter calculations for the volume velocity of a bandpass system. The pressure response would simply be ω times the results shown in that figure. Once again it is clear that ignoring the modes of the duct and enclosure can result in substantial errors.

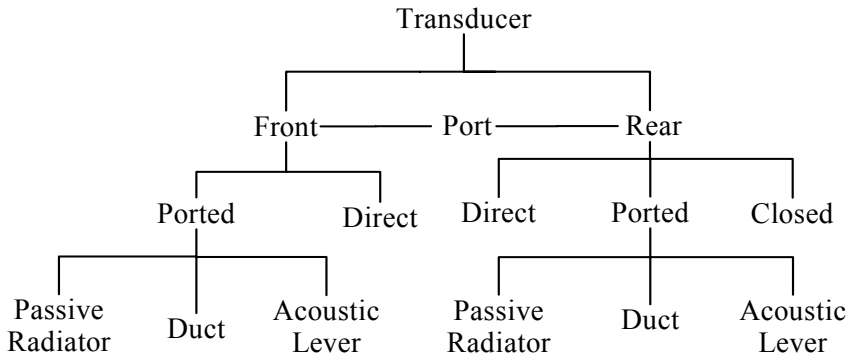
To summarize the results of this section, we have found that the T-matrix approach gives a better approximation and more analytical results than the lumped parameter approach. This is, however, a double-edged sword. While the results are more accurate, the added complexity of the T-matrix machinery can also obscure the more elegant results obtainable by the lumped parameter approach. With the full T-matrix approach, it is not possible to do tables of designs, monographs or simplified transfer functions, as is possible with lumped parameters. If T-matrices are to be used, then we must move away from the con-

cept of “alignments”. This leaves a dilemma that can only be resolved by the needs of the individual engineer.

A final consideration that we will discuss is that as enclosures become more and more complex the elegance of the lumped parameter approach begins to fail. This is true, for instance, for a double tuned bandpass system or a system with an Acoustic Lever™ where even the lumped parameter approaches yield equations that are too complex to allow for simple reductions to “alignments” or tables. Thus it seems clear that the domain for the effective use of the lumped parameter approach is relegated to the simpler systems, like the closed box, or single duct or passive radiator ported enclosures. As the complexity of the enclosure design increases, the need for an approach like T-matrices becomes ever more evident.

As regards this treatise, the above discussion makes clear that the classic analysis of loudspeaker enclosures, as is done in so many other texts, is of limited value to us. For this reason, we will describe enclosure concepts only in general terms realizing that to cover them in detail would require far more space than we have the time (or patience) for. Our objective here is to show alternative methods to the tried and true methods of Thiele and Small and not to review the fundamental results so well documented by our predecessors.

5.7 General Enclosure Types^{2,3}



The chart shown above lists the various types of enclosures that we could discuss. We will touch on them all but we will discuss only a few in any detail. In each case of a port, it can have one of three varieties of devices placed in it, each with its own characteristics. These devices are a duct (as in the previous section), a passive radiator, or an Acoustic Lever™⁴.

2. See Loudspeaker Anthology Vols. 1-4, *AES publications*
 3. See Beranek, *Acoustics*
 4. See Geddes, “The Acoustic Lever Enclosure”, *JAES*

This chart shows a myriad of possible combinations, more than a dozen, and these are only the first order systems. It is also possible to connect a port, with three variations between the front and rear enclosures for another entire set of combinations. By first order we mean a single enclosure-port combination. It is possible to link together an infinite number of first order sections (Helmholtz resonator), much like an electrical filter, to achieve an infinite number of combinations. We will stick to first order enclosures and only briefly mention those aspects of higher order devices that tend to make them less than optimal (in most cases).

We will go down the list, one by one, and discuss the need for further exploration or not. In most cases we will not go into any depth, mostly because the relevant details have already been covered.

Front – Direct, Rear – Direct

This enclosure is the simplest of all enclosures – basically no enclosure at all. Since the front and rear of the diaphragm are out of phase, this design is a dipole. The polar patterns that we have discussed before for monopoles (see Fig.4-2 on page 73) are still appropriate so long as they are multiplied by an additional $\cos(\theta)$ factor. This enclosure design is in fact more interesting than it first appears and can be quite useful. The response is mildly dependent on the size of the baffle for two reasons. The first is the dipole moment which affects the loading and the second is the diffraction of the baffle edge. To calculate the response taking into account the baffle diffraction can get quite complicated. Neither of these effects is of first order, however.

A critical point in our analysis is evident in the previous paragraph. We have referred to cabinet diffraction as a second order effect. Why we have classified it in this manner is important to understand. The first order effects are those that are an inherent characteristic of the transducer system. For instance, the effect of an enclosed volume is inherent with any closed box regardless of its shape. The diffraction, however is not. The shape of the enclosure is the dominate consideration for the diffraction. We know that minimizing the second derivative of the surface in which the transducer is placed will minimize the diffraction. So rounding the baffle edges will minimize the diffraction. Simply stated, we mean that no amount of study can reduce the effect of the enclosed volume, but judicious choice of enclosure shape, such as spherical, can virtually eliminate diffraction effects. First order effects are those that cannot be eliminated and must be understood in order to accommodate, Diffraction effects can be eliminated or diminished to a negligible amount.

Returning to the dipole enclosure, in order to minimize the diffraction the distance from the loudspeaker to the baffle edge should be varied as widely as possible and, as we said above, the baffle edges should be radiused (normal to the baffle). A transducer placed in the center of a donut (torroid) should be very effective at minimizing diffraction. Using these techniques the diffracted field will

be minimized to the point where it is negligible and can be ignored. In an optimized baffle the dipole has the directivity that we discussed above, but with one other feature. There is a transition of the summed volume velocity from a 4π steradian sound field at low frequencies to a 2π steradian sound field at high frequencies. The transition will occur at the point where the average distance from the front surface to the rear surface is

$$f = \frac{c}{\lambda_{avg}}$$

The more widely distributed the distances to the baffle edge are the more gradual this transition will be.

Front – Direct, Rear – Closed

We have already covered this design in some detail.

Front – Direct, Rear – Ported – Duct

This enclosure design has also already been covered using the T-matrix approach. Our intent, to show how to analyze them, has been served by the previous sections. It is worth mentioning that this enclosure can also be analyzed directly using the Wave Equation, just as we did for the closed box. The “port” is represented by a boundary condition on the opposite side of the sphere by, for example, a pressure release condition – a hole (a short duct). It is also possible to place an impedance value in this port representing, say, a passive radiator. It is unknown if any significant insights would be gained from this exercise. The reader is invited to try this as an interesting exercise.

Front – Direct, Rear – Ported – Passive Radiator

To first order, passive radiator systems work identical to ducts. If the acoustic mass of the passive radiator equals the acoustic mass of the duct and its compliance is negligible, then the two systems are virtually identical. There are several second order differences, however. The major difference in the two is that a passive radiator has much less physical velocity than a duct, given the usual situation of a passive radiator which has an area that is large compared with the area of the duct. This has several advantages. First, it lowers the losses due to viscosity effects in the duct and it lowers the generation of noise due to air turbulence. Of course a duct could be made as large as a passive radiator but then it would need to be very long, resulting in a total enclosure volume that would be much greater than that of the passive radiator. The real advantage of a passive radiator is its ability to get a high acoustic mass with a large cross sectional area in a relatively small space.

On the other hand, ducts are simple, inexpensive and with proper flaring, a smooth finish and sufficient area they can work quite well. The passive radiator can have nonlinearity in the suspension that will generate distortion if this suspen-

sion is too stiff. The audibility of passive radiator distortion has never been studied so its significance is really unknown.

It is easy to see from the T-matrix of a passive radiator that it is mathematically identical to a duct. The passive radiator has a T-matrix

$$\begin{bmatrix} \frac{1}{S_{pr}} & 0 \\ 0 & S_{pr} \end{bmatrix} \begin{bmatrix} 1 & -i\omega M_{pr} + R_{pr} + \frac{1}{-i\omega C_{pr}} \\ 0 & 1 \end{bmatrix} \begin{bmatrix} S_{pr} & 0 \\ 0 & \frac{1}{S_{pr}} \end{bmatrix} \quad (5.7.39)$$

which simplifies to

$$\begin{bmatrix} 1 & \frac{1}{S_{pr}^2} \left(-i\omega M_{pr} + R_{mpr} + \frac{1}{-i\omega C_{pr}} \right) \\ 0 & 1 \end{bmatrix} \quad (5.7.40)$$

S_{pr} = the area of the passive radiator,

M_{pr} = the passive radiators mechanical mass,

R_{pr} = the passive radiators mechanical resistance,

C_{pr} = the passive radiators mechanical compliance.

When the compliance term is negligible, which occurs if the passive radiators free air resonance is substantially below the box tuning frequency, then this form is identical to Eq.(5.3.27) for the lumped parameter duct. This comparison points out another major difference between the passive radiator and a duct – freedom from higher order modes.

Fig 5-14 shows a comparison between a passive radiator (solid) with a high compliance and one with a low compliance (dotted) (high compliance = ten times low compliance). A ported enclosure is also shown (dashed). For a sufficiently high compliance of the passive radiator, its response is indistinguishable from that of the duct. For a low compliance passive radiator, we do see a significant effect of the compliance term as a slight detuning of the system. This effect can be compensated for by a slight adjustment of the other parameters of the design. In essence, except for very small passive radiator compliance, the passive radiator and the duct work essentially identically. We must remember, of course, that we have considered the duct, in this case, to act as a lumped parameter port object – not a distributed pipe.

Front – Direct, Rear – Ported – Acoustic Lever™

We will discuss an Acoustic Lever™ in some detail since it is a relatively unique object with an interesting array of characteristics. Once we understand what an Acoustic Lever™ is and how it works. Then we will proceed to some examples.

An example of an Acoustic Lever™ is shown in Fig-5-15. The device appears to be much like a passive radiator, and acts somewhat the same. A lever has three

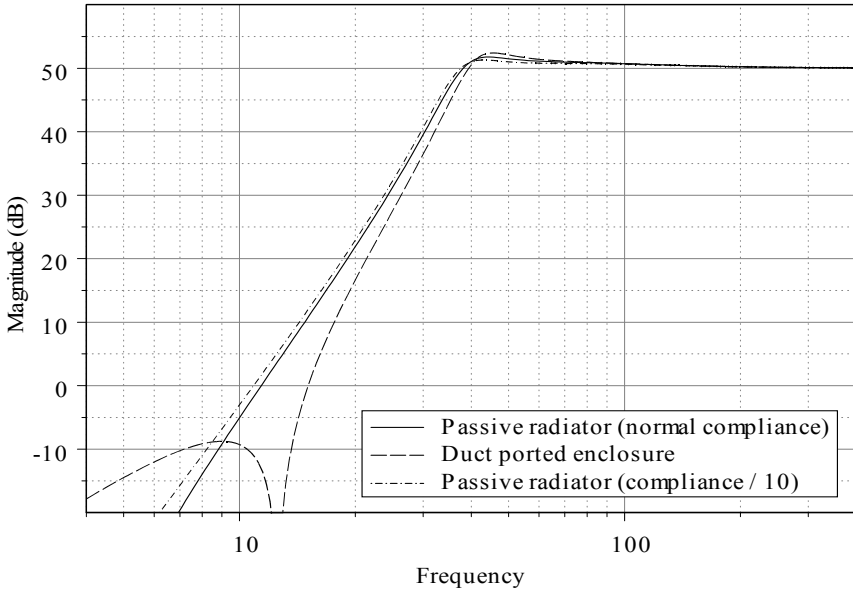


Figure 5-14 - Passive radiator with high and low compliance

physical areas that we need to consider: the driven area A_d , the radiating area A_r and the inner area, which is always $A_r - A_d$. Although the inner areas must always face some volume, it is easiest to understand the lever by ignoring this volume and considering it as part of the compliance of the lever. Made large enough, its effect can be made negligible. But it is this inner volume that is, in the end, the limiting factor to the performance of an Acoustic Lever™.

As a T-matrix the lever is quite simple

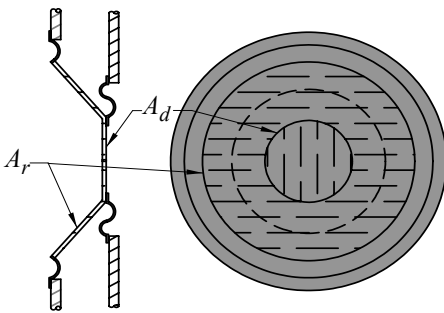


Figure 5-15 - An example of the construction of an Acoustic Lever™

$$\begin{bmatrix} \frac{1}{A_d} & 0 \\ 0 & A_d \end{bmatrix} \begin{bmatrix} 1 & -i\omega M_l + R_l + \frac{1}{-i\omega C_l} \\ 0 & 1 \end{bmatrix} \begin{bmatrix} A_r & 0 \\ 0 & \frac{1}{A_r} \end{bmatrix} \quad (5.7.41)$$

M_l = the levers mechanical mass,

R_l = the levers mechanical resistance,

C_l = the levers mechanical compliance (combined here with the acoustical compliance of the inner volume).

Multiplying out this matrix yields

$$\begin{bmatrix} \frac{A_r}{A_d} & \frac{1}{A_r A_d} \left(-i\omega M_l + R_l + \frac{1}{-i\omega C_l} \right) \\ 0 & \frac{A_d}{A_r} \end{bmatrix} \quad (5.7.42)$$

which is similar to the passive radiator matrix – equal to it, in fact – when the driven area equals the radiating area, as of course, it must be. We can write this matrix in another form which is perhaps more enlightening

$$\begin{bmatrix} 1 & \frac{1}{A_d^2} \left(-i\omega M_l + R_l + \frac{1}{-i\omega C_l} \right) \\ 0 & 1 \end{bmatrix} \begin{bmatrix} \frac{A_r}{A_d} & 0 \\ 0 & \frac{A_d}{A_r} \end{bmatrix} \quad (5.7.43)$$

which is exactly the same form as a passive radiator of area A_d with a transformer (electrical analog) placed at the output. A mechanical analog to a transformer is a lever – hence the name Acoustic Lever™.

It is well known that the power transfer through a transformer is constant. It neither creates or destroys energy, although a transformer can help to deliver more power to the load if there is an impedance mismatch between the input side and the output side, as is the case in enclosures for loudspeakers. To first order, we can simply think of a lever as a passive radiator, or a port, which amplifies the output volume velocity by the ratio of the radiating area to the driven area. By first order, here, we mean that we will ignore the radiation impedance and assume that the acoustical resistance and compliance of the lever are not significant. These later aspects can be problematic since the acoustical impedance of the lever as seen by the system is related to the smaller driven area, A_d , of the device, which tends to make these quantities larger than their equivalents in a passive radiator. Also, the acoustic mass, which is the mass that “tunes” the system, is also increased as the lever ratio increases. This means that in a very real sense, there is a practical limit to the kinds of gains that one can achieve with a lever. As the area ratio is increased for increased amplification, the acoustic values of all of the mechanical impedances for the lever go up. To maintain a constant acoustic mass

with increasing lever ratios one has to continually decrease the actual mechanical mass, which soon becomes impractical. This is also true of the resistance and the compliance. Ratios of 2:1 to about 4:1 are doable, 4:1 being the approximate practical limit, but even then, the actual construction of a robust 4:1 lever can become quite difficult.

When used with a direct radiating transducer, the lever can only be used to extend the bandwidth, not to increase the output. This is simply because the passband output of any direct radiating system is from the transducer itself. Therefore, the levers output cannot exceed that of the passband for a flat response. When tuned low the lever can have a substantial effect on the low frequency response, as shown in Fig.5-16. This plot shows a rear ported lever (dashed) along

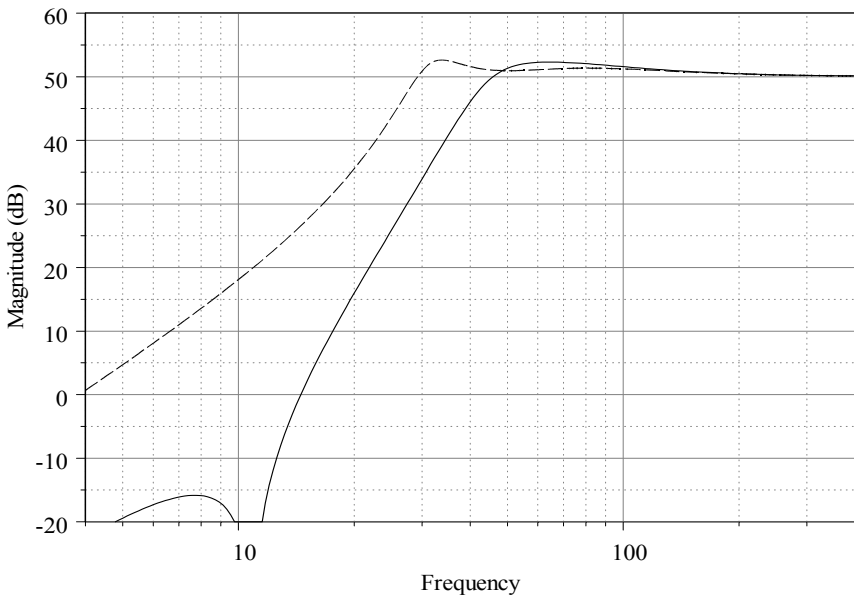


Figure 5-16 - Rear lever with direct radiator

with a rear ported passive radiator (solid). Both systems have a direct radiating transducer and both systems have the same box tuning. The lever and the passive radiator also have the same radiating area and the same acoustic mass. With a 2:1 lever ratio, the levers actual weight must be half as much as the passive radiator.

The response of the rear ported lever is quite good, but we must keep in mind that we have ignored the compliance of the lever's inner enclosure. Fig.5-17 shows the detrimental effect of reducing the lever compliance (smaller inner enclosure) and we can see that the net response is highly dependent on the compliance of the lever. As usual larger is better for low end performance.

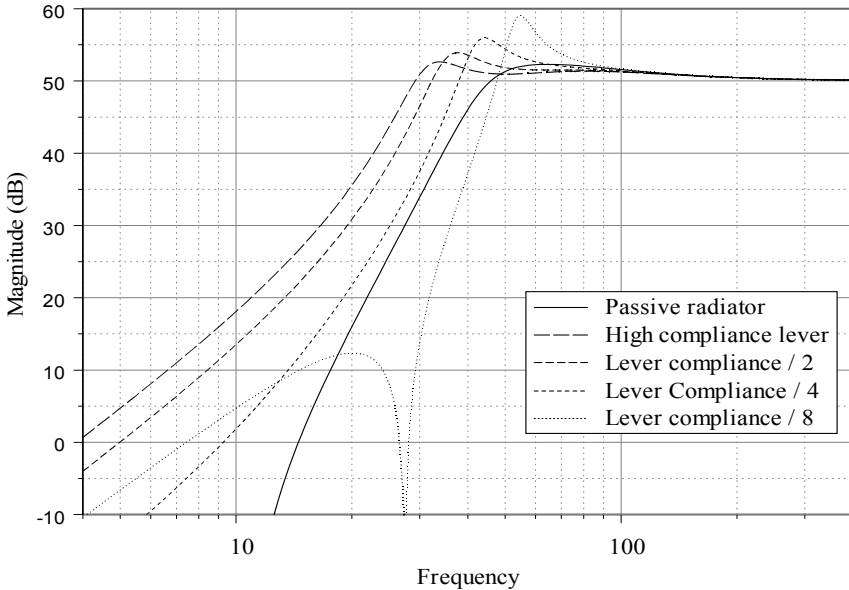


Figure 5-17 - Effect of lever compliance on response

Front – Ported, Rear – Direct

This is the same system as a Front–Direct, Rear–Ported system, in all cases.

Front – Ported – Duct, Rear – Closed

This enclosure design is probably third in common usage for low frequencies, following the closed box and rear ported designs. Its design is actually very straightforward. By tuning a Helmholtz resonator placed over the radiating transducer the efficiency of the system can be increased at the expense of bandwidth. This effect works essentially the same for any of the port elements: a lever, passive radiator or a duct. The increase in efficiency essentially comes from the higher impedance seen by the transducer in the region of the resonance of the front enclosure resonator. In the case of the Acoustic Lever™, the volume velocity is enhanced even further by the lever ratio.

Fig.5-18 shows a comparison of a ported system with three different elements in the port, a ducted, a passive radiator, and a 2:1 ratio lever. In each case, the front volume is tuned to the same frequency as the transducer when placed in its rear volume.

The basic characteristics of a front ported system are easily defined (to first order):

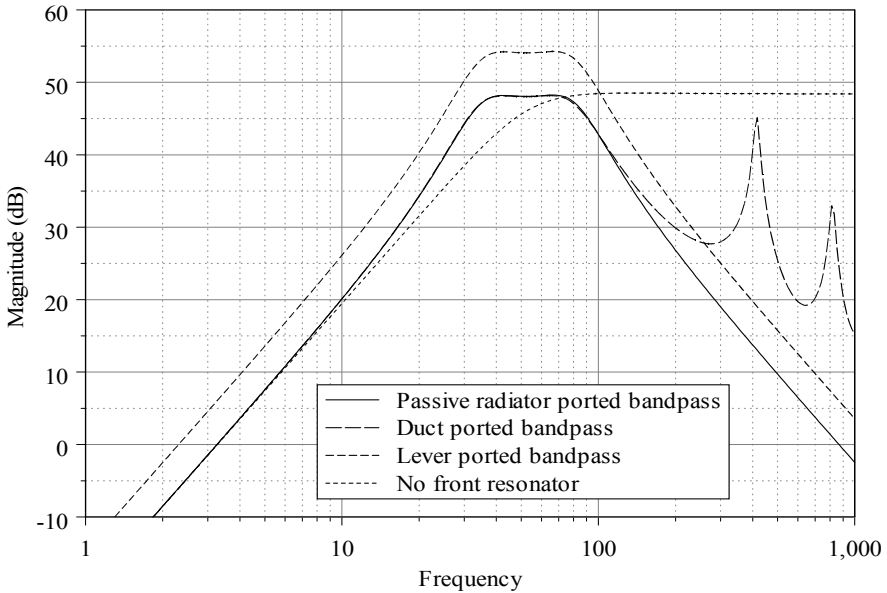


Figure 5-18 - Front ported, rear closed, enclosure with various port options

- The system is symmetric with its center frequency at the transducer's resonance (as enclosed in its rear box).
- The systems all require the same front volume and port acoustical mass for the same system Q .
- The duct and passive radiator yield virtually identical responses.
- The lever has an output that is increased in direct proportion to the lever ratio.
- Flat response occurs when the $V_{front} = Q_{total} V_{rear}$ where Q_{total} is the Q of the transducer in its rear volume.
- The bandwidth times efficiency is relatively constant (not mathematically in linear variables, but in a log-log sense).

The second order effects which have been ignored in the above analysis are simply the radiation load on the port objects and the internal resistances of the port objects. The effect of the lever's inner volume has also not been explicitly shown and it should be remembered that it does result in quite a substantial limitation of the output if allowed to shrink.

When the higher order effects are considered, the passive radiator tends to show a greater change in response from these parameters than the duct. The radiation load detunes the system to a slight degree, requiring a minor compensation with other component values. The system response can be greatly affected by the passive radiator's compliance and resistance if these values fall far from the opti-

mum. While neither of them can be eliminated altogether, they can usually be made to be insignificant.

The lever always has the greatest output, but when consideration is given to the compliance of the air between the lever surfaces it tends to result in a slightly larger system. The lever enclosure is always the limiting factor in using a lever and its effect is diminished only by increasing the “apparent” volume of this enclosure. It can be reduced in size with the use of a large amount of damping (completely stuffed in creasing the apparent volume), and further, experience has shown that small holes (for high damping) can be used to further reduce this volume without a substantial reduction in output from sound cancellation. The sound radiation from the holes is generally out of phase relative to the radiated pressure so the radiated pressure from the holes tends to reduce the total radiated sound pressure. Moving this “leakage” radiation as far away from the direct radiating lever as possible reduces this cancellation and in some applications (like automotive package tray subwoofer), this detrimental sound radiation can even be placed in non-coupling volume spaces (like the trunk). There are numerous ways to control the unwanted volume of the lever enclosure, and it is always best to consider the specifics of the application in doing this.

The radiation load tends to detune the Acoustic Lever™ system even more so than the passive radiator, i.e. the detuning is also magnified by the lever ratio.

Once the driver and rear volume are chosen the only variable is the Q of the front enclosure. This variable Q results from the fact that there are an infinite number of combinations of port and volume parameters that define a common resonance frequency. Each of these combinations will have a different Q and a

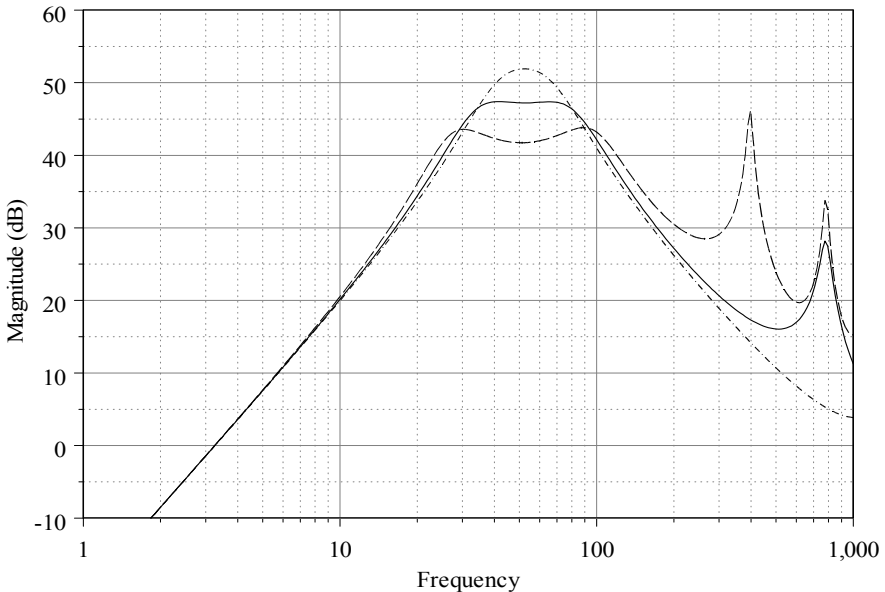


Figure 5-19 - Front duct chamber Q variation

different response curve. This effect is shown in Fig. 5-19 for a front ducted system. To first order all that is required for the design of a front ported system with a closed rear enclosure are a few simple rules, although detailed designs require either a simulation program or real world testing and tuning.

Front – Ported, Rear – Ported

In this section, we will investigate one of the more complex enclosure styles, namely a port on the front and the rear of the transducer enclosures.

With the possibility of three different port elements there are six unique combinations:

- duct and duct
- duct and passive radiator
- duct and lever
- passive radiator and passive radiator
- passive radiator and lever
- lever and lever

As we have already discussed, to a first order a duct and a passive radiator act the same. If we consider a duct and passive radiator to be synonymous, then there are only three unique combinations, and for all practical purposes only a dual passive radiator system really needs to be discussed.

Consider a transducer with two identical resonators on the front and rear diaphragm faces. The net radiation from these two resonators will be virtually zero except for the fact that the two ducts cannot occupy the same exact location and so there will always be some radiation depending on the dipole moment between the two exit ducts.

If now we slightly change the resonance frequencies of the two chamber then there will be a region between the two resonances that will have sound radiation which is clearly not zero since the phase shifts that result from the resonances will not allow for a complete cancellation of the radiation. Fig. 5-20 shows the impedance seen by the diaphragm as the two chambers are tuned apart. Note how with even a slight detuning of the system this impedance goes immediately from a very high resonance value to a very low anti-resonance value at the mid point.

Thus by slightly retuning an equal ported situation we should expect a rather large change in the effect of these two enclosures. This is in fact what happens, which can be seen in Fig. 5-21. Here we have a standard transducer in a box with two passive radiators on each end of a tube with a driver in a middle divider. The location of the divider is moved, changing the tuning of each resonator. The passive radiators are identical, which is not the correct relationship for a flat response. This figure demonstrates that as the tuning gets closer and closer to being equal the response falls. However, it is also apparent that the efficiency does reach a peak after which the volume shift simply extends the bandwidth. This occurs because the two ported enclosures are no longer tuned close enough together to act on each other. They become uncoupled. The response has

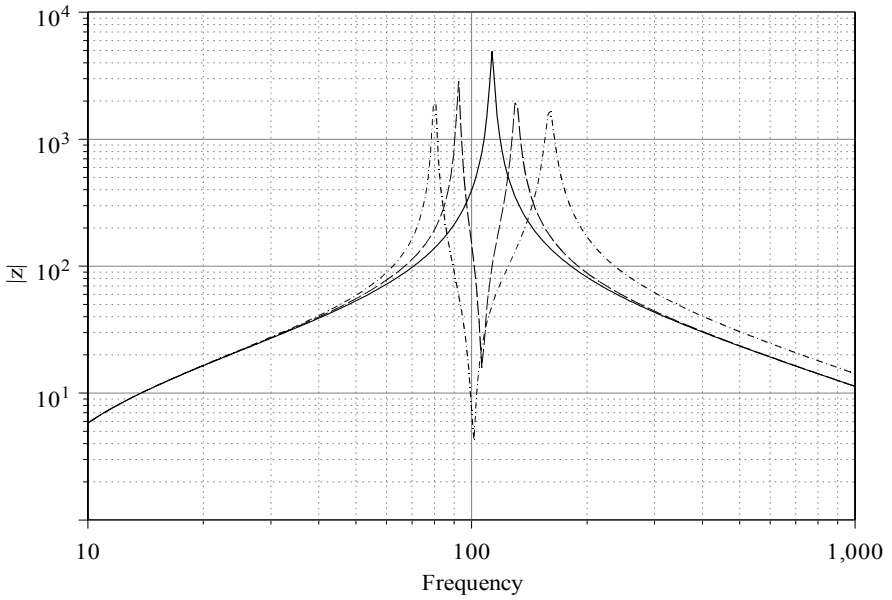


Figure 5-20 - Acoustical impedance on diaphragm from a dual ported system

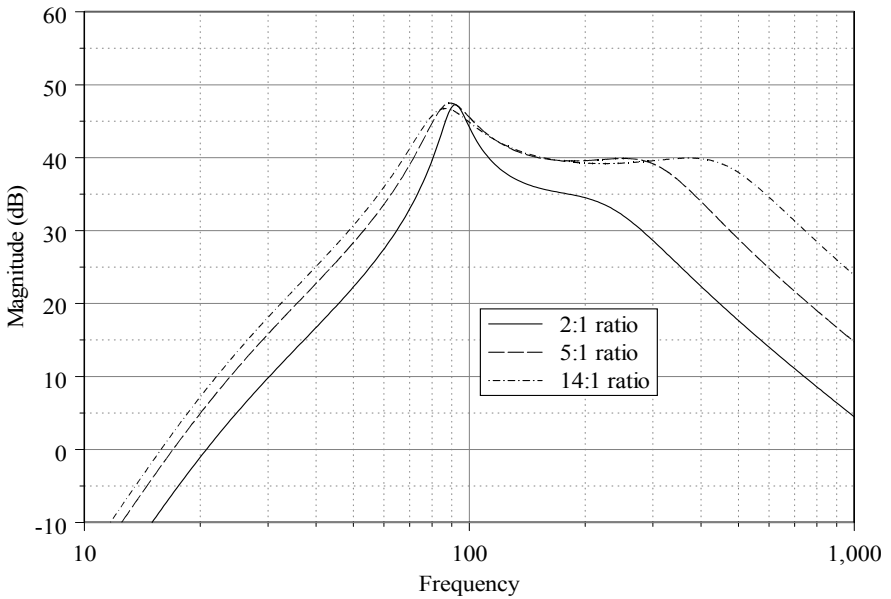


Figure 5-21 - Dual ported enclosure with movable interior baffle
(note that the total volume is constant)

become equivalent to a single ported system with an acoustic low pass filter on the other side of the diaphragm. Lets consider changing the tuning by adjusting the masses of the passive radiators instead of leaving the total volume constant and varying the ratio, as we just demonstrated.

Using equal volumes whose sum is the same as in the previous plot, and varying the tuning masses we obtain Fig.5-22. In this figure the product of the front

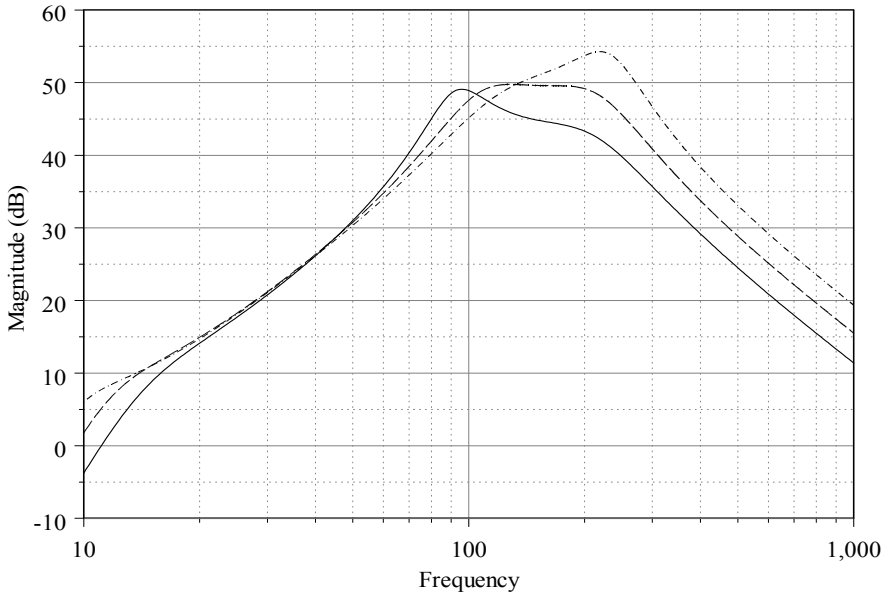


Figure 5-22 - Dual ported enclosure with tuning changes as passive radiator mass changes

and rear passive radiator masses has been made constant while varying the tuning. The volumes of the two chambers remain equal in all cases. Comparing Fig.5-21 and Fig.5-22 we can see that we basically tune the system with the masses while the volume ratio sets the bandwidth. Equal volumes yield the smallest bandwidth with the highest output.

Since the volumes and the masses both affect the response, it would be interesting to see the effect of retuning with different masses and volumes but with a constant set of tuning frequencies. This study is shown in Fig.5-23. This set of parameter changes basically modifies the gain of the response. The middle curves in the last two figures are identical systems.

The low frequency response of the lower curve in Fig.5-23 has some strange response irregularities. These are a result of the complex relative phase changes occurring at the lower resonance of the passive radiator subsystems. These irregularities are sensitive to response tuning and passive radiator parameters. They almost always stay well below the usable passband of the system.

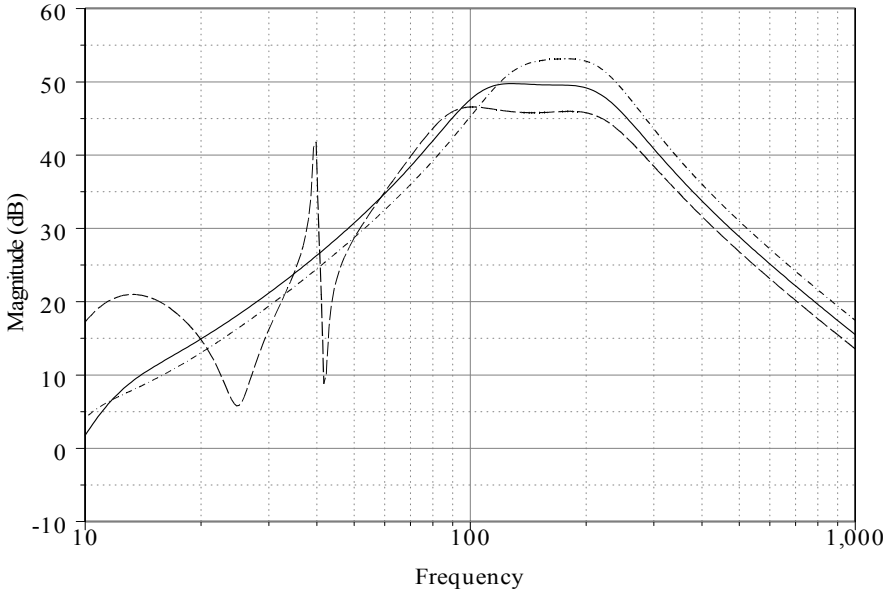


Figure 5-23 - Retuning with constant tuning frequencies

Tuning the dual bandpass system can be put into a few simple principles:

- The total volume sets the location of the center of the passband.
- The volume ratio sets the bandwidth.
- The masses of the ports tune the system for flat response.
- The ratio of the mass to compliance of the enclosures sets the gain.
- The transducer parameters of mass and compliance do not affect the problem to any appreciable degree, which is especially true for a high compliance unit with not too heavy of a cone.
- The system damping is almost completely controlled by the drivers' electromagnetic damping, making it the only important driver parameter for this type of system

In practice, these enclosures need a computer simulation to optimize, but in principle, they are not too difficult to design. Once again, the design (to a first order) is the same whether or not the ports are ducts, passive radiators (or as we shall see Acoustic Levers™). The details will differ between these different types of ports. However, the basic principles of tuning remain the same.

Now we must look at how the lever affects this more complex design. We will look at the same enclosure as in the previous graphs but with the passive radiators replaced with 2:1 levers of the same radiating area. The driver will also be the same. This will allow comparisons even though the absolute values here really have no meaning. It is the relative values that are significant.

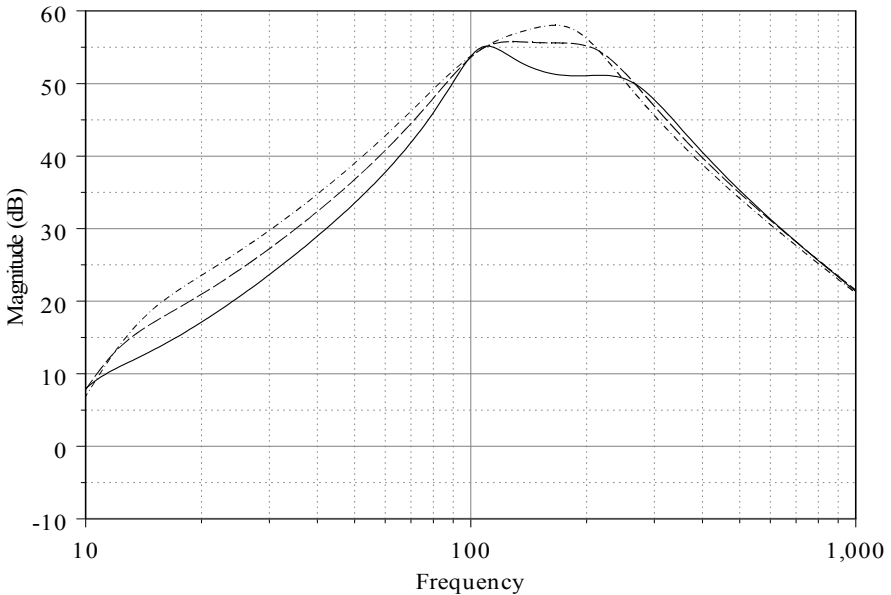


Figure 5-24 - Pressure response for a dual lever ported enclosure

Fig. 5-24 shows that the response tuning of the lever system is identical to that for a passive radiator. Of course, the actual mechanical lever masses will not be the same since here we have set the acoustical masses the same. The mechanical mass will be about half of that for the passive radiator. We have also ignored the lever enclosure when we talk about total volume. It is assumed to be large. Other than the lever enclosure (the volume between the lever surfaces), the lever works exactly like a passive radiator except it has a system gain which is proportional to the lever ratio.

The only remaining combination of dual ports that we have not discussed is a combination of a lever and a duct or passive radiator. There is no simple answer here as Fig. 5-25 shows. This figure has one of the levers replaced by a passive radiator. All of the other parameters remain identical to the previous figures, except for the passive radiator's area, which has been set equal to the inner (smaller) area of the lever.

While it is difficult to draw any substantial conclusions, the following can be noted for lever/non-lever dual ported enclosures:

- Replacing the low tuned lever does not make much difference implying that the use of two levers is unnecessary.
- Replacing the high tuned lever with a non-lever appears to lose all benefit. In the case of a large passive radiator area, the system would require substantial retuning to be useful.

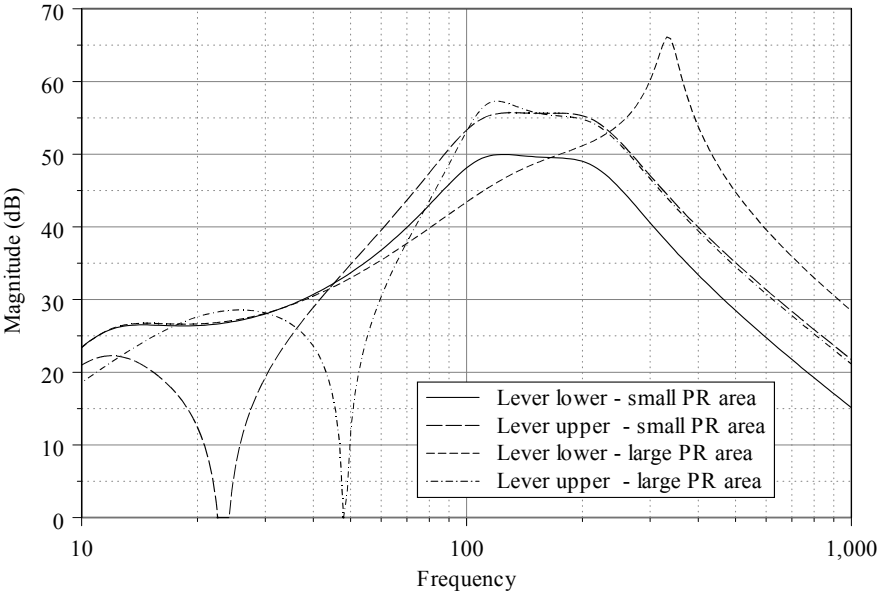


Figure 5-25 - Lever replaced with passive radiator of equal acoustic mass
(Note scale change)

Internal Ported

The last variation that we will describe is the internal ported system. This system is one in which the acoustic matrices cannot be reduced from the full form shown in Sec.5.5 on page 103. That is because of the coupling between the front and rear of the diaphragm. Eq.(5.5.34) needs to be modified as follows.

$$\begin{pmatrix} F_d \\ v_d \end{pmatrix} = \begin{bmatrix} S_d & 0 & -S_d & 0 \\ 0 & 1/S_d & 0 & 0 \\ 0 & 0 & 0 & -1/S_d \end{bmatrix} \begin{bmatrix} 1 & 0 & Z_c^{1,1} & Z_c^{1,2} \\ 0 & 1 & Z_c^{2,1} & Z_c^{2,2} \\ -Z_c^{1,1} & Z_c^{1,2} & 1 & 0 \\ Z_c^{2,1} & -Z_c^{2,2} & 0 & 1 \end{bmatrix} \begin{pmatrix} P_f \\ V_f \\ P_r \\ V_r \end{pmatrix} \tag{5.7.44}$$

Z_c = the coupling matrix between the front and the rear of the diaphragm

Eq.(5.7.44) has several assumptions built into it. The first is that the coupling matrix is symmetric with a determinate of one. This is always the case for a duct, but it is not true in general. The general case is too complex to consider here. We will look at the case of a single ported enclosure with a duct between the front and rear boxes. Eq.(5.7.44) then simplifies to

$$\begin{pmatrix} F_d \\ v_d \\ v_d \end{pmatrix} = \begin{bmatrix} S_d & 0 & -S_d & 0 \\ 0 & 1/S_d & 0 & 0 \\ 0 & 0 & 0 & -1/S_d \end{bmatrix} \cdot \begin{bmatrix} 1 & 0 & \cos(kl) & \frac{-i\rho c}{A}\sin(kL) \\ 0 & 1 & \frac{A}{i\rho c}\sin(kL) & \cos(kl) \\ -\cos(kl) & \frac{-i\rho c}{A}\sin(kL) & 1 & 0 \\ \frac{A}{i\rho c}\sin(kL) & -\cos(kl) & 0 & 1 \end{bmatrix} \cdot \begin{bmatrix} 1 & -i\omega M_{af} & 0 & 0 \\ -i\omega C_{abf} & 1-\omega^2 C_{abf} M_{af} & 0 & 0 \\ 0 & 0 & 1 & 0 \\ 0 & 0 & -i\omega C_{abr} & 1 \end{bmatrix} \begin{pmatrix} P_f \\ V_f \\ P_r \\ V_r \end{pmatrix} \quad (5.7.45)$$

C_{abf} = front box acoustic compliance

C_{abr} = rear box acoustic compliance

M_{af} = front duct acoustic mass

L = length of internal duct

A = area of internal duct

In the low frequency regime this simplifies to

$$\begin{pmatrix} F_d \\ v_d \\ v_d \end{pmatrix} = \begin{bmatrix} \omega^2 M_{ad} C_{abr} S_d & (-i\omega^3 M_{ad} M_{af} C_{abf} + i\omega M_{ad}) S_d & \omega^2 M_{ad} C_{abr} S_d \\ \frac{-i\omega C_{abf}}{S_d} & \frac{1-\omega^2 M_{af} C_{abf}}{S_d} & \frac{-i\omega(C_{ad} + C_{abr})}{S_d} \\ \frac{-i\omega(C_{ad} + C_{abf})}{S_d} & \frac{1-\omega^2 M_{af}(C_{ad} + C_{abf})}{S_d} & \frac{-i\omega C_{abr}}{S_d} \end{bmatrix} \cdot \begin{pmatrix} P_f \\ U_f \\ P_r \end{pmatrix} \quad (5.7.46)$$

C_{ad} = the acoustic compliance of the internal duct

M_{ad} = the acoustic mass of the internal duct

Following the exactly the same procedure as before we can eliminate P_r by using the third equation in the two above. Then noting that terms in P_f are negligible (why?) we finally get

$$\begin{pmatrix} F_d \\ v_d \end{pmatrix} = \begin{pmatrix} (-i\omega^3 M_{ad} M_{af} (C_{abf} + C_{abr}) + i\omega M_{ad}) S_d \\ \frac{1 - \omega^2 (M_{af} (C_{ad} + C_{abf} + C_{abr}))}{S_d} \end{pmatrix} \cdot V_f \quad (5.7.47)$$

which is an attractively simple result. It is now a simple matter to multiply the left side by the electromechanical terms representing the transducer from which we could solve for the output ports volume velocity for either a voltage source, a current source or and combination thereof. This example was shown simply to develop the technique but its results are not interesting enough to warrant further development here. This task is left to the reader.

5.8 Summary

We have shown in this chapter how the T-matrix approach can be used to develop the solution to virtually any enclosure problem no matter how complex. These results can be simplified to yield the classical lumped parameter results or they can be numerically calculated for a level of detail that is unavailable with lumped parameter techniques. Of the numerous enclosure variations that we have looked at, no one stands out as being ideal, they all have trade-offs. For an unconstrained design for maximum output however, the Acoustic Lever™ is the clear choice.